ACS SyntheticBiology

pubs.acs.org/synthbio Research Article

Macroscopic Assembly of Materials with Engineered Bacterial Spores via Coiled-Coil Interaction

Published as part of ACS Synthetic Biology special issue "Materials Design by Synthetic Biology".

Lucas Korbanka, Ju-An Kim, and Seunghyun Sim*

Cite This: *ACS Synth. Biol.* 2024, 13, 3668−3676 Read Online

ACCESS | Metrics & More | Article Recommendations | Supporting Information

ABSTRACT: Herein, we report macroscopic materials formed by the assembly of engineered bacterial spores. Spores were engineered by using a T7-driven expression system to display a high density of pH-responsive self-associating proteins on their surface. The engineered surface protein on the spore surface enabled pH-dependent binding at the protein level and enabled the assembly of granular materials. Mechanical properties remained largely constant with changing pH, but erosion stability was pH-dependent in a manner consistent with the pH-dependent interaction between the engineered surface proteins. Our finding utilizes synthetic biology for the design of macroscopic materials and illuminates the impact of coiled-coil interaction across various length scales.

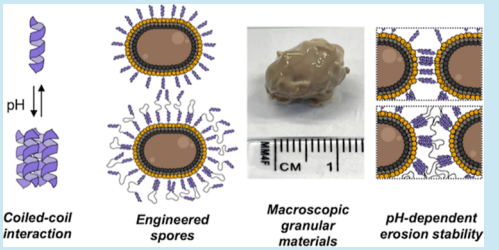

KEYWORDS: *coiled-coil interaction, engineered spores, granular materials, erosion stability*

INTRODUCTION

Biology provides key insights for engineering materials.[1−3] Complex morphologies and functions in natural biological materials, such as wood, are genetically encoded functionalities. Advanced tools in the field of synthetic biology have been accelerating the development of new materials, and examples include the work of Joshi and colleagues, who successfully engineered *Escherichia coli* to express biofilms with designer properties such as metal adhesion or protein binding.[4] Ajo-Franklin and co-workers' work demonstrates macroscopic materials autonomously formed by proteins expressed and secreted from engineered strains of bacteria.[5] Developing and expanding new fundamental knowledge and design rules across length scales, from protein−protein interaction to macroscopic properties of materials, remains an important challenge in the field of engineered living materials.

Protein assembly programs the hierarchical structures and physical properties of natural biological materials. Self-assembling bacterial amyloid proteins confer features such as adhesion and resistance to naturally occurring biofilms.[6] In animals, essential structural proteins such as keratin and collagen are both formed by an assembly of proteins.[7] The coiled-coil motif is one of the most fundamental and common protein self-assembly motifs found in nature.[8] The sequence−structure relationship of coiled coils is well understood and has enabled computational designs of many synthetic coiled coils.[9] Researchers have employed coiled coils to create stimulus-responsive hydrogels and tunable colloidal assemblies.[10−15] Bacterial surfaces decorated with coiled-coil motifs were shown to modulate the adhesion of bacteria to yield cellular aggregates in the mesoscale.[16,17] We envisioned that these well-understood interactions can be used to arrive at macroscopic materials comprising cellular building blocks. To date, the macroscopic assembly of materials comprising cellular building blocks mediated by coiled-coil interactions is unprecedented.

Bacterial spores are useful biological building blocks for designing robust materials operating under abiotic conditions. Unlike living cells that require nutrients and hydrated environments, spores are dormant, partially dehydrated, and can withstand harsh environments such as high temperatures, desiccation, ultraviolet irradiation, chemical insults, and long-term dehydration.[18] When returned to favorable growth conditions, vegetative cells germinated from spores can be used to grow more spores or carry out a genetically encoded function.[18,19] Sahin and co-workers demonstrated the superior mechanical response of *Bacillus subtilis* spores to water gradients and successfully used them to create micron-scale biohybrid hygromorph actuators.[20] In another work, Voigt and co-workers embedded *B. subtilis* spores into a material resilient to environmental stresses, which could be germinated to realize various engineered functionalities.[19] Recently, we developed a T7 ribonucleic acid (RNA) polymerase-enabled high-density

Received: July 2, 2024
Revised: October 3, 2024
Accepted: October 7, 2024
Published: October 11, 2024

https://doi.org/10.1021/acssynbio.4c00468
ACS Synth. Biol. 2024, 13, 3668−3676

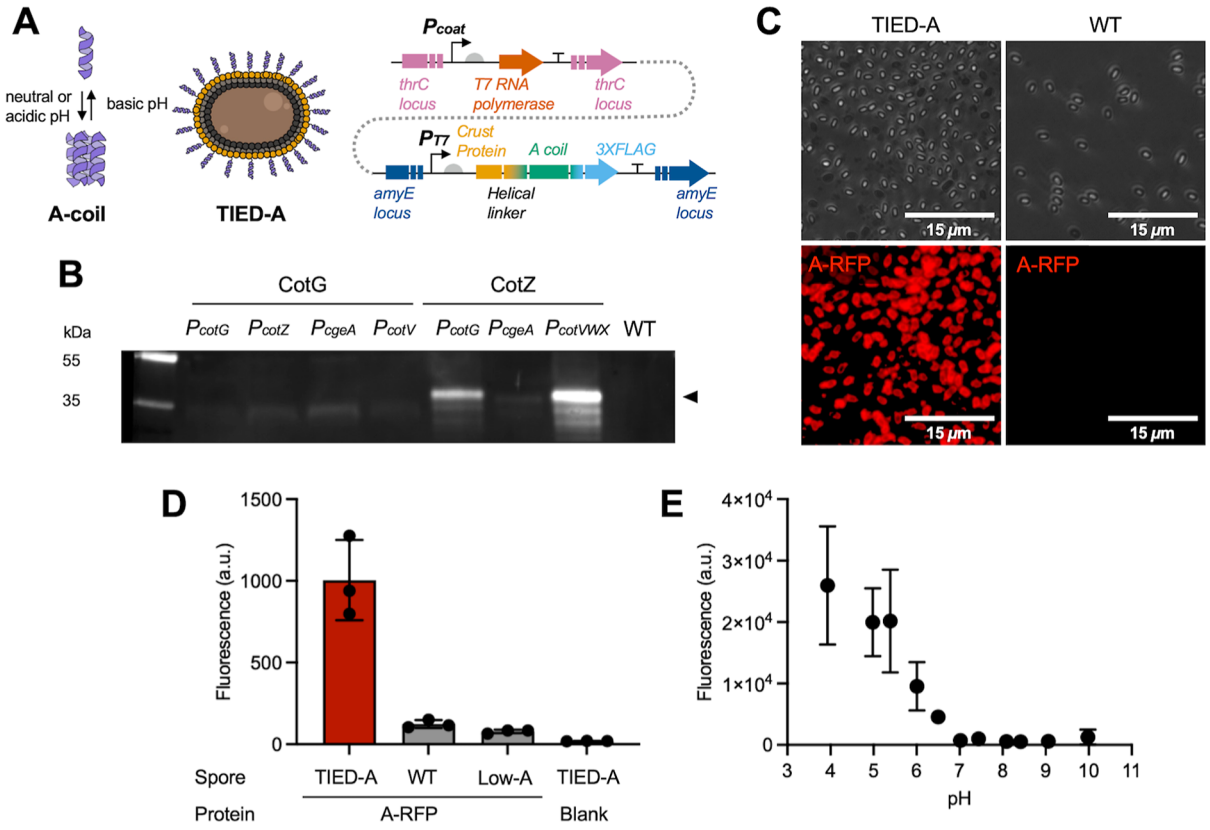

Figure 1. Construction of TIED-A spores. (A) General design of engineered genetic circuits in this study. P_{coat} promoters active in the late stages of sporulation drive the expression of the highly active T7 RNA polymerase, which subsequently transcribes A-coil fusion proteins. (B) Western blot images of the spore proteome of the selected colonies after double transformation. Coat proteins are resolved by SDS-PAGE and transferred for Western blot analyses with primary mouse anti-FLAG and secondary goat antimouse Alexa-Fluor-647-conjugated antibody. Protein concentrations were normalized by OD_{600} of the spores used to prepare the lysate. (C) Phase contrast (top) and fluorescence (bottom) microscopy images of engineered spores incubated with A-RFP (1.0 mg/mL A-RFP with OD_{600} = 0.7 spores in PBS, pH 6.9, 22 °C, 250 rpm, 2.75 h) and subsequently washed by spinning down at 4000*g* for 15 min and resuspended in fresh PBS two times. (D) Bulk fluorescence measurements taken after fluorescent labeling of the spores with A-RFP (1.0 mg/mL A-RFP with OD_{600} = 0.7 spores in PBS, pH 6.9, 22 °C, 250 rpm, 2.75 h) and subsequent washing by spinning down at 4000*g* for 15 min four times. (E) Bulk fluorescence measurements of A-RFP-bound spores at various pHs. N = 3 replicates. Mean ± standard deviation.

protein display (TIED) system for bacterial spores, achieving loading densities of 10^6–10^7 enzymes per spore.[21] TIED spores showed stress-tolerant catalytic activity, and the use of bacterial spores as biocatalysts allowed for catalyst renewal by germination to a vegetative state followed by sporulation.[21] Our subsequent work used synthetic polymers to assemble these spores into catalytic macroscopic materials.[22]

In this study, we demonstrated the formation of macroscopic materials with engineered bacterial spores displaying a coiled-coil motif. High concentrations of self-associating coiled-coil proteins on the spore surface were enabled by the TIED system.[21] Stimulus-responsive protein–protein interactions were confirmed via binding studies with fluorescent protein probes and were used in the formation of macroscopic materials. We also engineered spores displaying a telechelic protein with a coiled-coil motif to understand the effect of varying protein architectures on the resulting material property. We tested these materials' mechanical properties and their pH dependence, determining that our materials show a pH-dependent erosion stability attributed to the engineered surface protein.

RESULTS

Construction of TIED-A Spores. Motivated by the potential of *B. subtilis* spores as a building block for durable, long-lasting, and stimulus-responsive biocomposite materials, we set out to engineer the spore surface with a stimulus-responsive protein–protein interaction motif. A small protein, referred to as "A-coil", was chosen because of its small size (4.8 kDa), antiparallel aggregation, simple secondary structure, and ability to refold after being heated to a fully denatured state.[10,11,14,15] At near neutral pHs and moderate temperatures, A-coil forms an α helix, which reversibly assembles into antiparallel tetramers using a leucine zipper motif.[11,14,23] Tirrell and co-workers showed that at suitably high concentrations, telechelic proteins comprising A-coils at the chain ends form temperature- and pH-responsive hydrogels.[10,11,14,15]

We elected to use the TIED system to achieve a high density of A-coil on the spore surface.[21] A complete TIED genetic circuit works by engineering *B. subtilis* to express the T7 RNA polymerase during the late stages of sporulation. This highly active polymerase then drives the overexpression of spore coat fusions of a desired protein, which assembles onto the spore surface. We chose to display proteins using the TIED system as TIED can achieve a higher concentration of proteins on spores than other spore display techniques. We empirically

https://doi.org/10.1021/acssynbio.4c00468
ACS Synth. Biol. 2024, 13, 3668–3676

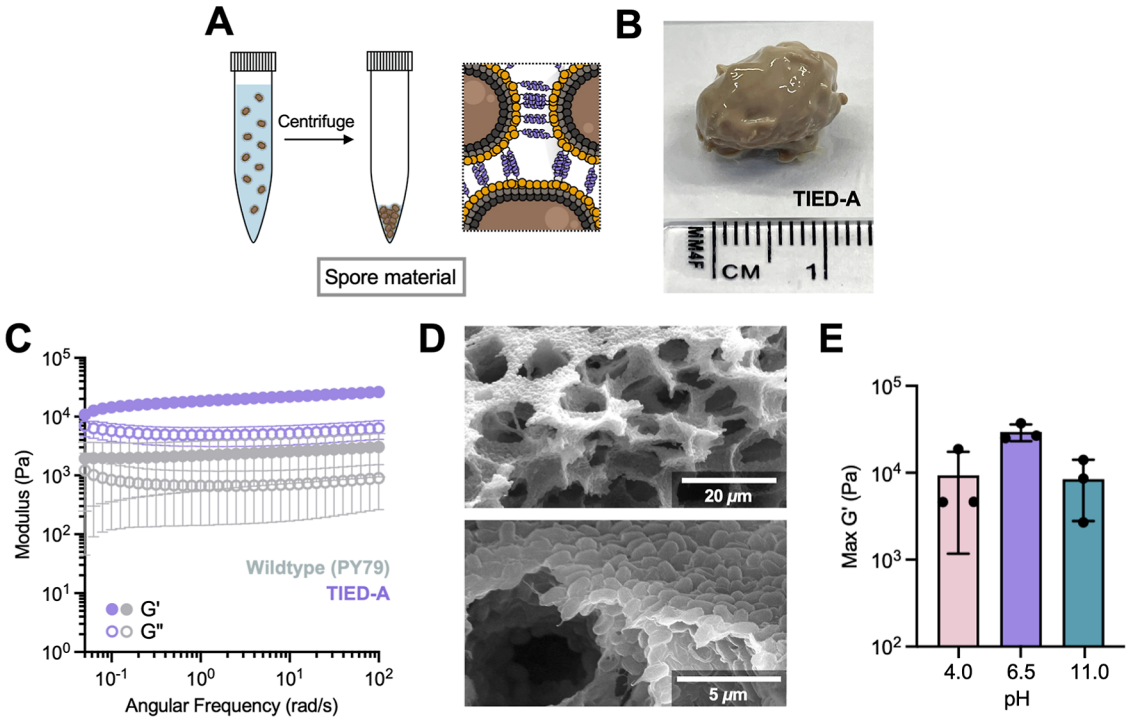

Figure 2. Assembly of TIED-A spores into macroscopic materials. (A) Schematic illustration of the TIED-A material synthesis procedure. Spores from 1 L cultures suspended in 30 mL of PBS (pH 4.0, 6.5, or 11.0) were pelleted by excessive centrifugation (first 4000*g* for 30 min at 22 °C, then 21,130*g* for 12−18 h). After pipetting off the supernatant, 200 μL of fresh PBS buffer was added to the pellet to allow removal of spore materials. (B) Representative photographic image of TIED-A materials. (C) Storage moduli G' (filled circles) and loss moduli G'' (open circles) of TIED-A and wild-type spore materials prepared at pH 6.5. (D) Scanning electron microscopy (SEM) images of lyophilized TIED-A hydrogels at low (top) and high (bottom) magnifications. (E) Maximum G' of TIED-A materials prepared at various pHs. $N = 3$ biological replicates. Mean ± standard deviation.

determined the best combination of promoter sequences and coat protein fusion partners for the high expression of A-coil fusion proteins by the sequential double transformation (Figure 1A). Spores were then made by following an early harvest sporulation protocol to maximize the density of intact spore coat fusions.[21] Western blot of the spore coat proteome with FLAG tag antibody revealed that the P_{CotG}−CotZ and P_{CotVWX}−CotZ promoter and fusion partner combinations showed a high expression of the CotZ-fused A-coil on the spore surface (Figure 1B). The P_{CotVWX}−CotZ combination was selected for further studies due to the apparent higher expression and is hereafter referred to as TIED-A. Comparison with a previously reported TIED construct revealed a similar expression level for the TIED-A (Figure S3).[21] The complete TIED-A genetic circuit was verified by whole genome sequencing. All the combinations of tested promoters with the CotG fusion protein yielded a low expression. The whole genome sequencing of the P_{CotG}−CotG combination revealed the missing T7 amplification part at the *thrC* locus despite double antibiotic selection. We elected this strain as a low-expressing control (Low-A) to assess the impact of T7-mediated amplification.

Having established that TIED-A displays a high density of A-coils on the spore surface, we sought to verify that the A-coil is functional and behaves as expected. TIED-A spores were incubated with an mRFP fluorophore fused with A-coil (A-RFP) in PBS (137 mM NaCl, 2.7 mM KCl, 10 mM Na_2HPO_4 1.8 mM KH_2PO_4, pH 6.9). After unbound A-RFP was washed, fluorescent microscopy images of spores showed surface localization of A-RFP on the TIED-A spore surface but not on wild-type (PY79) spores (Figure 1C). The bulk fluorescence intensity of these spore suspensions corroborated these images and revealed that the high density of A-coil on spores is critical to observe the intended coiled-coil interaction, as the wild-type and Low-A spores resulted in low fluorescence emission from the bound A-RFP (Figure 1D).

We then investigated whether the unique pH dependence of the interaction between A-coils is maintained in the TIED-A spores. Bulk fluorescent measurements with A-RFP at different pHs showed that TIED-A spores interact with A-RFP at pHs lower than 7 (Figure 1E), consistent with previous reports on the pH response of this protein.[10] We note that errors in this experiment are relatively large in low pH samples due to the engineered spores' tendency to stick to surfaces at low pH, leading to unavoidable loss of spores during the washing procedure (Figure S4).

Assembly of TIED-A Spores into Macroscopic Materials. Based on our fluorescence microscopy results suggesting that TIED-A forms pH-dependent coiled-coil interactions, we hypothesized that TIED-A spores at sufficiently high concentrations could assemble into pH-tunable macroscopic materials. We first concentrated TIED-A spores suspended in PBS at pH 6.5 into a spore pellet by centrifugation. This pH was selected based on the expected formation of a protein−protein interaction, while avoiding potential complications associated with surface protein precipitation at low pH. This concentrated suspension was difficult to remove and characterize. However, we observed that by pipetting additional buffer (200 μL PBS, pH 6.5) around the interface between the tube and the material, the material became detached from the tube

https://doi.org/10.1021/acssynbio.4c00468
ACS Synth. Biol. 2024, 13, 3668−3676

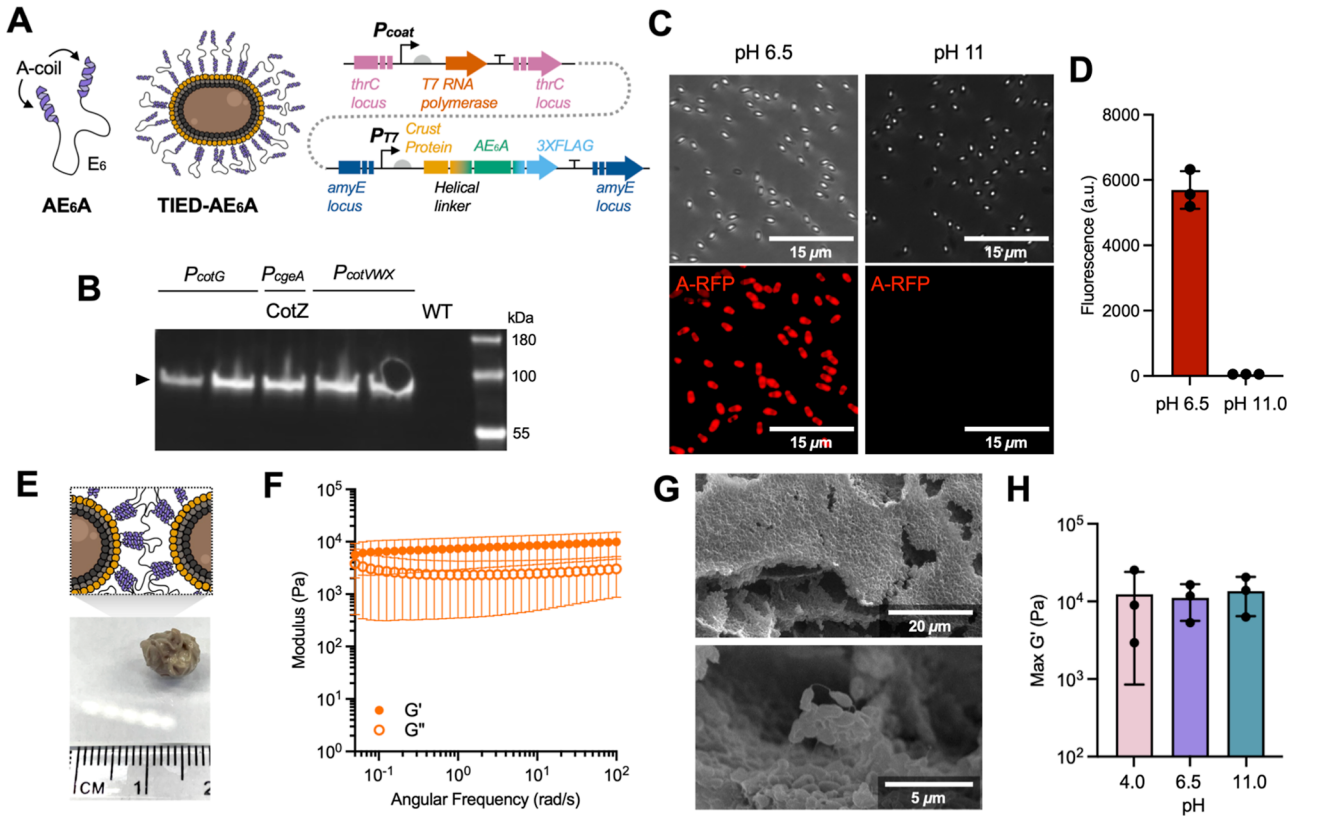

Figure 3. TIED-AE$_6$A spore: design, characterization, and assembly of macroscopic materials. (A) Schematic illustrations of AE$_6$A protein (left), TIED-AE$_6$A (middle), and genetic constructs to obtain TIED-AE$_6$A (right). A telechelic AE$_6$A protein that forms hydrogels was displayed on the spore surface, yielding TIED-AE$_6$A spores. (B) Western blot images of the spore proteome. Coat proteins are resolved by SDS-PAGE and transferred for Western blot analyses with primary mouse anti-FLAG and secondary goat antimouse Alexa-Fluor-647-conjugated antibody. Protein concentrations were normalized by OD_{600} of the spores used to prepare the lysate. (C) Phase contrast (top) and fluorescence (bottom) microscopy images of the TIED-AE$_6$A spores incubated with A-RFP (1.0 mg/mL A-RFP with OD_{600} = 0.7 spores in PBS pH 6.5 or 11.0, 22 °C, 250 rpm, 2.75 h) and subsequently washed with by spinning down at 4000*g* for 15 min, removing the supernatant, and resuspending in fresh PBS pH 6.5 or 11.0 two times. (D) Bulk fluorescence measurements of TIED-AE$_6$A spores labeled with A-RFP at two different pHs (1.0 mg/mL A-RFP with OD_{600} = 0.7 spores in PBS, pH 6.5 or 11.0, 22 °C, 250 rpm, 2.75 h) after washing by spinning down at 4000*g* for 15 min four times. (E) Schematic illustration and a representative photographic image of TIED-AE$_6$A materials. (F) G' and G'' of TIED-AE$_6$A spore materials. (G) SEM images of lyophilized TIED-A materials at low (top) and high (bottom) magnifications. (H) Maximum G' of TIED-AE$_6$A materials at various pHs. N = 3 biological replicates. Mean ± standard deviation.

surface and could be easily removed, yielding a cohesive, elastic, and self-standing macroscopic material (Figure 2A,B). The viscoelastic property of the TIED-A materials (Figure 2C) and materials prepared from wild-type spores (Figure 2C) was probed by frequency-sweep measurement. Both materials are viscoelastic solids, and TIED-A materials showed a slightly higher storage modulus (G') in all tested frequency ranges (Figure 2C). We were surprised to find that wild-type spore materials had a measurable mechanical property, given the lack of any engineered self-associating surface protein. In light of our result, we reasoned that both the TIED-A and wild-type materials, being composed of highly concentrated spores, are best classified as granular materials packed into a jammed state. Granular materials are materials composed of systems of particles with diameters greater than a micron.[24−26] Spores are approximately 1−1.5 μm in diameter (Figures 1C and 3C). At high concentrations, granular materials can enter a jammed state, where the particles are closely packed and the bulk property transitions from liquid-like to solid-like.[26] In granular materials, gravity is a greater contributor to particle motion than thermal agitation, and friction is more important than van der Waals interaction in understanding the forces between particles.[26] As such, the bulk mechanical properties of these materials would be primarily determined by particle size, shape, and stiffness, which explains the similarity between TIED-A and wild-type spore materials.[27,28] While both systems behave as viscoelastic solids, the surface interaction between A-coils on spores likely increased the stiffness of the resulting materials in TIED-A samples.

The structure of TIED-A materials was probed with SEM. SEM images of the lyophilized TIED-A materials showed an assembly of spores interrupted by large pores, presumably from water escape from the network during the freeze-drying process (Figure 2D, top). At larger magnifications, fracture sites around the pores revealed fibrillar structures extending from the TIED-A spores, leaving behind fibers of disconnected matter (Figure 2D, bottom). SEM images of wild-type spore materials revealed a similar structure (Figures S10 and S11). Another notable feature of the TIED-A spores in the SEM images is that the boundaries of individual spores were weakly defined. We then tested the pH response of TIED-A materials by preparing them at pH 11.0 and pH 4.0. Our results showed a slight decrease in maximum G' for both pHs (Figure 2E). The result did not follow the trend observed from the A-RFP

https://doi.org/10.1021/acssynbio.4c00468
ACS Synth. Biol. 2024, 13, 3668−3676

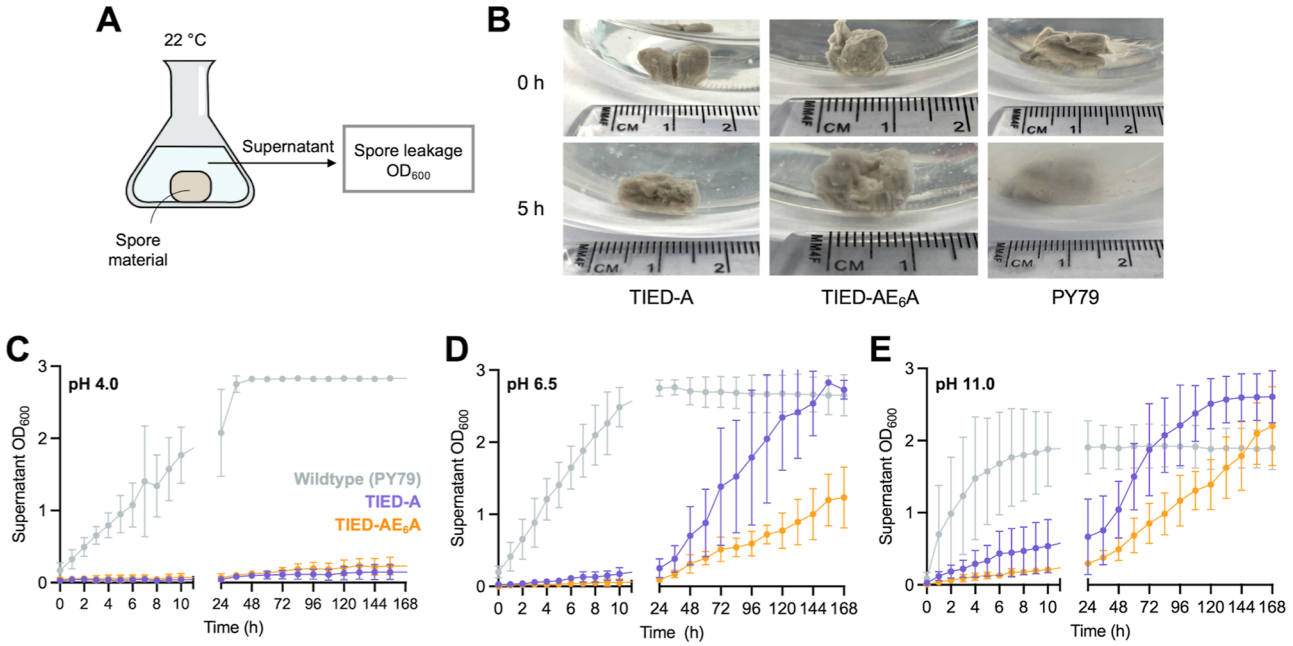

Figure 4. Erosion stability of TIED-A and TIED-AE$_6$A materials. (A) Schematic of the erosion assay. Spore materials prepared at a certain pH are added to PBS at that pH to a concentration of 5 mg material/mL PBS, and the supernatant OD_{600} is measured to track spore leakage. (B) Representative images of materials taken at 0 and 5 h for the pH 6.5 assay. (C) OD_{600} trace of the supernatant in the pH 4.0 erosion assay for TIED-A, TIED-AE$_6$A, or wild-type spore materials (22 °C) over the course of 1 week. (D) OD_{600} trace of the supernatant at pH 6.5 containing TIED-A, TIED-AE$_6$A, or wild-type spore materials (22 °C) over the course of 1 week. (E) OD_{600} trace of the supernatant at pH 11.0 containing TIED-A, TIED-AE$_6$A, or wild-type spore materials (22 °C) over the course of 1 week.

binding study probing the protein-level pH-dependent interaction (Figure 1C). Wild-type materials prepared at pH 4.0 and 11.0 showed maximum G' values similar to TIED-A, though none as high as TIED at pH 6.5 (Figures S18−S21).

TIED-AE$_6$A Spore: Design, Characterization, and Assembly of Macroscopic Materials. We then investigated the effect of the self-associating protein's structure on the resulting material properties. Telechelic systems of A-coils have been studied extensively and found to form pH- and temperature-responsive hydrogels.[10,11,15,23] Telechelic AE$_6$A protein (28.5 kDa) bears two A-coils flanking 6 repeats of the E chain derived from elastin. Several TIED-AE$_6$A constructs were made with the CotZ protein fusion partner and a few promoter sequences (Figure 3A). Western blot analysis of the spore coat proteome verified that all three constructs successfully expressed a high density of the CotZ-AE$_6$A fusion protein on the spore surface (Figure 3B). The P_{CotVWX}−CotZ combination was selected as TIED-AE$_6$A for further studies because TIED-A also uses the P_{CotVWX}−CotZ promoter and fusion partner, allowing for direct comparison between the two. The complete TIED-AE$_6$A genetic circuit was verified by whole genome sequencing.

Similar to TIED-A, TIED-AE$_6$A also binds to A-RFP, as evidenced by fluorescence localization on the spore surface (Figure 3C) and increased bulk fluorescence emission (Figure 3D) at pH values lower than 7. At a high pH (pH 11.0), TIED-AE$_6$A failed to form a robust interaction with A-RFP, indicating that the intended pH response of the coiled-coil interactions operates on the surface of TIED-AE$_6$A spores.

When making materials using the same procedure as for TIED-A at pH 6.5, the TIED-AE$_6$A spores yielded cohesive, elastic, and self-standing macroscopic materials (Figure 3E), with a storage modulus slightly lower than that of TIED-A prepared under the same conditions (Figure 3F). This result suggests that the additional A-coils on the telechelic AE$_6$A proteins are not contributing to the network stiffness, possibly due to the formation of intramolecular loops rather than interspore A-coil interactions or due to the additional length between interacting A proteins. SEM images of the lyophilized TIED-AE$_6$A materials showed structural features similar to those of TIED-A (Figure 3G, top). Similar to TIED-A, the general mechanical properties of TIED-AE$_6$A did not change at various pHs (Figure 3H). We again reason that these materials are best classified as granular materials packed into a jammed state with the bulk material properties largely determined by particle size, shape, and stiffness.

pH-Dependent Erosion Stability of TIED-A and TIED-AE$_6$A Materials. In contrast to our initial expectation that these materials would have different mechanical properties at different pHs due to the pH-dependent binding of A-coil to TIED-A and TIED-AE$_6$A, we observed generally similar G' values across the tested pHs, many of which were not different from the wild-type, a result which can be understood when considering the nature of granular materials. However, throughout the mechanical testing, we observed that TIED-A and TIED-AE$_6$A seemed more cohesive than materials prepared with wild-type spores. Previous reports by Tirrell and co-workers investigated the erosion stability of telechelic protein hydrogels, finding the effect of topology of self-associating proteins on erosion rate.[11] We thus hypothesized that TIED-A and TIED-AE$_6$A might show enhanced erosion stability compared to wild-type materials due to the engineered surface A-coils cohesively holding the material together.

TIED-A, TIED-AE$_6$A, and wild-type spore materials were immersed in PBS at various pH values (Figure 4A). At pH 4.0, TIED-A and TIED-AE$_6$A both showed minimal spore leakage and material erosion over the course of 7 days compared to the wild-type, which disassembled quickly upon immersion (Figure

https://doi.org/10.1021/acssynbio.4c00468
ACS Synth. Biol. 2024, 13, 3668−3676

4B). At pH 6.5, TIED-A showed significant improvement over the wild-type, with limited erosion for the first 24 h of the assay, followed by steady spore leakage over the next few days (Figure 4C,D). Interestingly, TIED-AE_6A at pH 6.5 showed erosion stability better than that of both the wild-type and TIED-A (Figure 4D). At pH 11.0, both TIED-A and TIED-AE_6A showed improvement over the wild-type but eroded more quickly than in lower-pH experiments (Figure 4E). This result generally mirrors the trend observed in our A-RFP binding study and suggests that the engineered surface protein is able to improve the erosion stability of these jammed spore materials at low pH where the protein−protein interaction is occurring. TIED-AE_6A showed erosion slower than that of TIED-A at pH 6.5 and 11.0 (Figure 4D,E). We speculate that the higher number of protein−protein interaction domains (Figure S3) contributes to these observed differences. Low-A showed slightly better erosion stability than the wild-type at pH 4.0 but was not as stable as TIED-A or TIED-AE_6A (Figure S25). At pH 6.5 and 11.0, Low-A was not erosion-stable. This result supports that a higher number of protein−protein interaction domains on the spore surface lead to greater erosion stability.

To demonstrate the potential utility of our system for practical application, we tested whether the materials formed by the engineered spores could release an embedded cargo in a pH-responsive manner (Figure S21). A-RFP, a model cargo, was incorporated into TIED-AE_6A spore materials and released more rapidly at pH 9.0 than at pH 4.0. This proof-of-concept experiment suggests that our engineered spores could be used to deliver protein cargo in a pH-responsive manner.

DISCUSSION

We developed a new approach to making macroscopic materials via the assembly of engineered *B. subtilis* spores displaying a high density of stimulus-responsive and self-associating proteins. A-coil and telechelic AE_6A protein was translationally fused to the CotZ *B. subtilis* coat protein and displayed on the spore surface. These proteins remain functional and recruit other A-coils to the spore surface in a pH-dependent manner. Upon centrifugation, TIED-A and TIED-AE_6A spores assembled into macroscopic materials and exhibited pH-dependent erosion stability.

This work is the first example of a macroscopic material assembled entirely from engineered *B. subtilis* spores alone. As such, it outlines a generalizable platform and illuminates some design considerations for arriving at more sophisticated future generations of materials comprising engineered cells or spores. Because our engineered spores enable the delivery of protein cargo in a pH-responsive manner, future work could utilize this platform for the oral delivery of protein biologics. Engineered TIED spores, in particular, show great potential for building robust materials for practical applications, as they bypass the cell viability and biotic condition requirements for materials encasing living cells. It may be possible to realize materials with different and superior mechanical properties by employing stronger protein−protein interaction motifs on the TIED spores.

We originally anticipated creation of materials with pH-tunable mechanical properties via the use of stimulus-responsive A-coil proteins; however, we ultimately arrived at materials that showed broadly similar mechanical properties. We reasoned that our materials are best classified as granular materials that have been packed into a jammed state and that material properties were, therefore, predominantly determined by the shape, size, and stiffness of the spores rather than the engineered surface protein.[26−28] Intended protein−protein interaction on the engineered spore surface led to pH-dependent erosion stability, a result that provides useful insight to future researchers regarding which properties could be tunable or altered in similar systems. The fact that our materials remained intact and exhibited similar mechanical properties at pHs far outside the realm of what most cells can tolerate suggests that TIED spore materials may have practical applications in circumstances in which other engineered biological materials are unable to persist due to the harsh environment. We believe that future materials composed of TIED spores bearing protein−protein interaction domains will realize a wide variety of engineered properties and serve many practical applications.

METHODS

Design and Cloning of Genetic Constructs and Transformation into *B. subtilis*. The A and AE_6A gene sequences were obtained from Sim lab stock and amplified using colony PCR. The fragments were then cloned using Golden Gate (for A) or Gibson Assembly (for AE_6A) into PBS1C plasmids for T7-driven expression of CotZ/CotG coat protein fusions. All flanking sequences were identical to a previously reported construct.[21] TIED-A and TIED-AE_6A were constructed by following a previously reported double transformation protocol.[21] TIED-A and TIED-AE_6A constructs were verified using a whole genome sequencing service (Plasmidsaurus, GenBank: CP159912 and CP159874). Additional cloning details are available in Supporting Information.

General Spore Preparation. The spores used in this study were prepared similar to the previous report[21] but with the following modifications. Two 5 mL precultures were grown in Lysogeny broth (5 μg/mL chloramphenicol) until saturation, rather than to the mid-exponential phase, and were then inoculated to 1 L of LB media and grown 20−24 h at 250 rpm, 37 °C before sporulation. Sporulation and lysis were carried out as described previously using 250 mL of PBS and 15 mL of 1 mg/mL lysozyme in PBS for each 1 L culture. After lysis, the spore pellet was resuspended in 30 mL of PBS at the desired pH for further use.

Decoating of Spores and Western Blot of Spore Coat Proteome. The previously reported decoating procedure was followed,[21] with the following changes. 1 mL of spores (OD_{600} = 1.0) in PBS was spun down at 4000*g* for 10 min and resuspended in 500 μL of decoating buffer. Spores were then heated for 30 min at 65 °C, followed by probe sonication on ice (1 s on, 1 s off, at 100% intensity for 30 s total) and heating at 65 °C for an additional 10 min. The decoated spores were separated from the solubilized spore coat proteome by centrifugation at 10,000*g* for 15 min. 15 μL of solubilized spore coat proteome was then combined with 5 μL of 4x Laemmli buffer with 0.4 M DTT and heated at 95 °C for 5 min. 10 μL of the resulting samples was used for SDS-PAGE gel electrophoresis and run at 222 V for 24 min. Subsequent gel imaging, immunostaining, and western transfer were all carried out according to the established methods.[21]

Design and Cloning of A-RFP Fusion Protein. A-coil and mRFP sequences were directly amplified from bacterial colonies using colony PCR with overhanging restriction sites. The PCR fragments were then purified by using gel

https://doi.org/10.1021/acssynbio.4c00468
ACS Synth. Biol. 2024, 13, 3668−3676

electrophoresis and cut with restriction enzymes. The digested product was purified by using the Qiagen gel extraction kit to remove enzymes and short DNA fragments. The PCR fragments were then ligated into a linearized pQE80 plasmid using the M0202 protocol from New England Biolabs. The ligation mixture was then transformed into DH10B electrocompetent cells (New England Biolabs, C3019) and plated on an antibiotic plate (carbenicillin 100 μg/mL). Successful transformation of the correct construct was verified by using Sanger sequencing (Azenta). The plasmid was then purified and transformed into electrocompetent BL21(DE3) using electroporation and checked via colony PCR. Additional cloning details are provided in the Supporting Information.

A-RFP Expression and Purification. BL21(DE3) bearing the pQE80 A-RFP plasmid was streaked onto an LB agar plate (100 μg/mL carbenicillin) and grown for 14 h at 37 °C. A single colony was then inoculated into 1 L of Terrific Broth. The culture was grown for 8 h at 250 rpm, 37 °C. The OD_{600} was monitored by using a NanoDrop One UV−vis spectrophotometer. Protein expression was induced after 8 h at OD_{600} = 0.6 by adding 1 mL of 1 M filter-sterilized isopropyl β-D-1-thiogalactopyranoside. Induction was carried out for 18 h at 25 °C, 120 rpm. Cells were harvested by centrifugation at 4000*g*, 4 °C, for 20 min. The supernatant was poured off and the pellets frozen at −80 °C. The pellet was then thawed on ice and resuspended in 40 mL of lysis buffer (50 mM NaH_2PO_4, 300 mM NaCl, and 10 mM imidazole, pH 8) with 1 mg/mL lysozyme from chicken egg white (Sigma-Aldrich no. 6876-5G). Once resuspended, the mixture was left on ice for an additional 30 min. The lysis mixture was separated into six 15 mL centrifuge tubes, which were sonicated on ice. The lysates were then centrifuged at 40,000*g*, 4 °C, for 30 min. 30 mL of Ni-NTA agarose resin slurry (Qiagen no. 30210) was added to the soluble fraction and rocked gently at room temperature in the dark for an hour. The entire mixture was then subjected to affinity column chromatography. SDS-PAGE gel electrophoresis was used to examine protein identity and purity. After dialysis, the protein was flash-frozen at −80 °C and lyophilized into a dry powder.

A-RFP pH-Dependent Labeling Assay. Spore solutions were prepared in PBS at various pHs (OD_{600} = 0.7) and mixed with A-RFP (1.0 mg/mL) at 22 °C and 250 rpm for 2 h and 43 min. After consecutive washing with PBS at various pHs (137 mM NaCl, 2.7 mM KCl, 10 mM Na_2HPO_4, 1.8 mM KH_2PO_4, and pH 3.10, 3.93, 4.98, 5.39, 6.01, 6.50, 7.02, 7.44, 8.09, 8.42, 9.06, and 9.98), bulk fluorescence was measured using the plate reader (BioTek Synergy H1, excitation: 550 nm, emission: 610 nm). We note that below pH 7, OD_{600} decreased substantially due to their tendency to stick to surfaces and each other.

A-RFP Labeling Assays with an Optical and Fluorescence Microscope. The spores prepared analogously to the pH-dependent binding study were subjected to phase contrast and fluorescence imaging. 0.6 μL of the labeled spore suspension was pipetted onto a 2% agarose pad on a glass slide, covered with a glass coverslip, and imaged. All fluorescent images (excitation 560/40, emission 630/75) were taken with identical imagining conditions to ensure fair comparison.

Spore Material Preparation. TIED-A or TIED-AE_6A spores were prepared.[21] The resuspended pellet in 30 mL of PBS (137 mM NaCl, 2.7 mM KCl, 10 mM Na_2HPO_4, 1.8 mM KH_2PO_4, and pH 3.97, 6.53, or 10.97) was spun down at 4255*g* and 22 °C for 30 min in a 50 mL conical tube. The supernatant was poured off, leaving a soft sticky pellet behind. The pellets were further concentrated by pipetting 1.5 mL of pellet into 1.7 mL microcentrifuge tubes and spinning down at 21,130*g*, removing any supernatant, and adding more spore pellet to the microcentrifuge tube until a pellet volume of ∼900 μL was obtained. The pellets were then spun down at 21,130*g* for an additional 16 h. Any remaining supernatant was removed, and then, 200 μL of PBS (137 mM NaCl, 2.7 mM KCl, 10 mM Na_2HPO_4, 1.8 mM KH_2PO_4) at the desired pH was added back to the tube. The PBS was gently pipetted up and down along the edges of the tube to allow the material to detach from the surface of the tube. The material could then be removed from the tube by swirling with a pipet tip, tweezers, or a spatula for further experimentation and analysis. Identical steps were taken for wild-type spores.

Rheological Characterization of TIED-A and TIED-AE_6A Materials. Rheology was performed on a Discovery series HR-3 rheometer from TA Instruments using a cone and plate geometry (40 mm, 2° cone, TA Instruments no. 511406.905) and TRIOS software. Frequency sweeps from 0.05 to 600 rad/s were carried out at 0.1% strain at 25 °C. To minimize changes in material properties due to water evaporation, ∼10 mL of water was pipetted around the sample pedestal, and a custom 3D-printed chamber was placed over both the pedestal and geometry to maintain a humid environment throughout the experiments.

Scanning Electron Microscopy of TIED-A and TIED-AE_6A. TIED-A and TIED-AE_6A materials were lyophilized and mounted to a stub using double-sided conductive adhesive tape. The samples were then sputter-coated and imaged using a TESCAN GAIA3 SEM-FIB.

pH-Dependent Erosion Stability Assays. Spore materials were prepared using PBS (137 mM NaCl, 2.7 mM KCl, 10 mM Na_2HPO_4, 1.8 mM KH_2PO_4) at the tested pH (4.0, 6.5, or 11.0). After weighing each material (mass ranged from 213 to 959 mg), they were washed with PBS at the tested pH and then placed into PBS buffer at the tested pH to a concentration of 5 mg spore material/mL PBS. The differences in the final OD_{600} for these experiments were likely caused by material loss during the transfer process. The materials were then shaken at 22 °C, 250 rpm, for 40 s to mix the solution and suspend any spores that had leaked from the material. 1 mL of supernatant was then removed, and the OD_{600} was measured on a NanoDrop spectrophotometer using a cuvette. The samples were stored at 22 °C, 0 rpm, and the OD_{600} was checked using the same technique every hour for the first 10 h and then every 12 h after the first day.

■ ASSOCIATED CONTENT

Supporting Information

The Supporting Information is available free of charge at https://pubs.acs.org/doi/10.1021/acssynbio.4c00468.

Materials; instrumentation; genetic constructs; cloning details; full Western blot data; spore labeling data including bulk fluorescence data for additional washes and OD_{600} of TIED-A at various pHs; SEM images of TIED-A, TIED-AE_6A, and wild-type spore materials; rheological results of individual replicates for frequency sweeps of TIED-A, TIED-AE_6A, and wild-type materials at different pHs and wild-type material maximum modulus; and supplementary experiments including engineered spore germination studies, pH-responsive

https://doi.org/10.1021/acssynbio.4c00468
ACS Synth. Biol. 2024, 13, 3668−3676

release of embedded cargo, and erosion stability of Low-A (PDF)

AUTHOR INFORMATION

Corresponding Author

Seunghyun Sim − *Department of Chemistry, University of California Irvine, Irvine, California 92697, United States; Department of Chemical and Biomolecular Engineering, Department of Biomedical Engineering, and Center for Synthetic Biology, University of California Irvine, Irvine, California 92697, United States;* orcid.org/0000-0002-4232-5917; Email: s.sim@uci.edu

Authors

Lucas Korbanka − *Department of Chemistry, University of California Irvine, Irvine, California 92697, United States*

Ju-An Kim − *Department of Chemistry, University of California Irvine, Irvine, California 92697, United States*

Complete contact information is available at: https://pubs.acs.org/10.1021/acssynbio.4c00468

Author Contributions

L.K. designed, performed, and analyzed the experiments. L.K. wrote the manuscript. J.A.K. performed the experiments. S.S. designed the study and wrote the manuscript.

Notes

The authors declare no competing financial interest.

ACKNOWLEDGMENTS

This work is supported by the UC Irvine start-up fund. The research reported in this publication was also supported by the National Institute of General Medical Sciences of the National Institutes of Health under award number R35GM150770. The content is solely the responsibility of the authors and does not necessarily represent the official views of the National Institutes of Health. This research was partially supported by the National Science Foundation Materials Research Science and Engineering Center program through the UC Irvine Center for Complex and Active Materials (DMR-2011967). J.A.K. was supported by Allergan and UROP fellowship from UC Irvine. The authors acknowledge the use of facilities and instrumentation at the UC Irvine Materials Research Institute (IMRI) supported in part by the National Science Foundation Materials Research Science and Engineering Center program through the UC Irvine Center for Complex and Active Materials (DMR-2011967).

REFERENCES

(1) Gilbert, C.; Ellis, T. Biological Engineered Living Materials: Growing Functional Materials with Genetically Programmable Properties. *ACS Synth. Biol.* **2019**, *8* (1), 1−15.

(2) Sim, S. Network Formation of Engineered Proteins and Their Bioactive Properties. In *Engineered Living Materials*; Springer, 2022; pp 1−26.

(3) Molinari, S.; Tesoriero, R. F.; Ajo-Franklin, C. M. Bottom-up approaches to engineered living materials: Challenges and future directions. *Matter* **2021**, *4* (10), 3095−3120.

(4) Nguyen, P. Q.; Botyanszki, Z.; Tay, P. K. R.; Joshi, N. S. Programmable biofilm-based materials from engineered curli nanofibres. *Nat. Commun.* **2014**, *5* (1), 4945.

(5) Molinari, S.; Tesoriero, R. F.; Li, D.; Sridhar, S.; Cai, R.; Soman, J.; Ryan, K. R.; Ashby, P. D.; Ajo-Franklin, C. M. A de novo matrix for macroscopic living materials from bacteria. *Nat. Commun.* **2022**, *13* (1), 5544.

(6) Wang, X.; Zhang, S.; Zhang, J.; Wang, Y.; Jiang, X.; Tao, Y.; Li, D.; Zhong, C.; Liu, C. Rational design of functional amyloid fibrillar assemblies. *Chem. Soc. Rev.* **2023**, *52*, 4603−4631.

(7) Shoulders, M. D.; Raines, R. T. Collagen Structure and Stability. *Annu. Rev. Biochem.* **2009**, *78* (1), 929−958.

(8) Liu, J.; Rost, B. Comparing function and structure between entire proteomes. *Protein Sci.* **2001**, *10* (10), 1970−1979.

(9) Woolfson, D. N. The design of coiled-coil structures and assemblies. *Adv. Protein Chem.* **2005**, *70*, 79−112.

(10) Petka, W. A.; Harden, J. L.; McGrath, K. P.; Wirtz, D.; Tirrell, D. A. Reversible hydrogels from self-assembling artificial proteins. *Science* **1998**, *281* (5375), 389−392.

(11) Shen, W.; Zhang, K.; Kornfield, J. A.; Tirrell, D. A. Tuning the erosion rate of artificial protein hydrogels through control of network topology. *Nat. Mater.* **2006**, *5* (2), 153−158.

(12) Olsen, B. D.; Kornfield, J. A.; Tirrell, D. A. Yielding behavior in injectable hydrogels from telechelic proteins. *Macromolecules* **2010**, *43* (21), 9094−9099.

(13) Dooling, L. J.; Tirrell, D. A. Engineering the dynamic properties of protein networks through sequence variation. *ACS Cent. Sci.* **2016**, *2* (11), 812−819.

(14) Shen, W.; Kornfield, J. A.; Tirrell, D. A. Dynamic properties of artificial protein hydrogels assembled through aggregation of leucine zipper peptide domains. *Macromolecules* **2007**, *40* (3), 689−692.

(15) Shen, W.; Kornfield, J. A.; Tirrell, D. A. Structure and mechanical properties of artificial protein hydrogels assembled through aggregation of leucine zipper peptide domains. *Soft Matter* **2007**, *3* (1), 99−107.

(16) Veiga, E.; Lorenzo, V. d.; Fernández, L. A. Autotransporters as Scaffolds for Novel Bacterial Adhesins: Surface Properties of *Escherichia coli* Cells Displaying Jun/Fos Dimerization Domains. *J. Bacteriol.* **2003**, *185* (18), 5585−5590.

(17) Kozlowski, M. T.; Silverman, B. R.; Johnstone, C. P.; Tirrell, D. A. Genetically programmable microbial assembly. *ACS Synth. Biol.* **2021**, *10* (6), 1351−1359.

(18) McKenney, P. T.; Driks, A.; Eichenberger, P. The Bacillus subtilis endospore: assembly and functions of the multilayered coat. *Nat. Rev. Microbiol.* **2013**, *11* (1), 33−44.

(19) González, L. M.; Mukhitov, N.; Voigt, C. A. Resilient living materials built by printing bacterial spores. *Nat. Chem. Biol.* **2020**, *16* (2), 126−133.

(20) Chen, X.; Mahadevan, L.; Driks, A.; Sahin, O. Bacillus spores as building blocks for stimuli-responsive materials and nanogenerators. *Nat. Nanotechnol.* **2014**, *9* (2), 137−141.

(21) Hui, Y.; Cui, Z.; Sim, S. Stress-Tolerant, Recyclable, and Renewable Biocatalyst Platform Enabled by Engineered Bacterial Spores. *ACS Synth. Biol.* **2022**, *11* (8), 2857−2868.

(22) Kawada, M.; Jo, H.; Medina, A. M.; Sim, S. Catalytic Materials Enabled by a Programmable Assembly of Synthetic Polymers and Engineered Bacterial Spores. *J. Am. Chem. Soc.* **2023**, *145* (29), 16210−16217.

(23) Zehner, N. A.; Dietrick, S. M.; Tirrell, D. A.; Kennedy, S. B. Two-Site Internally Cooperative Mechanism for Enzyme Kinetics in a Hydrogel Forming Recombinant Protein. *Biomacromolecules* **2015**, *16* (11), 3651−3656.

(24) de Gennes, P. G. Granular matter: a tentative view. *Rev. Mod. Phys.* **1999**, *71* (2), S374−S382.

(25) Qazi, T. H.; Muir, V. G.; Burdick, J. A. Methods to Characterize Granular Hydrogel Rheological Properties, Porosity, and Cell Invasion. *ACS Biomater. Sci. Eng.* **2022**, *8* (4), 1427−1442.

(26) Riley, L.; Schirmer, L.; Segura, T. Granular hydrogels: emergent properties of jammed hydrogel microparticles and their applications in tissue repair and regeneration. *Curr. Opin. Biotechnol.* **2019**, *60*, 1−8.

(27) Qazi, T. H.; Wu, J.; Muir, V. G.; Weintraub, S.; Gullbrand, S. E.; Lee, D.; Issadore, D.; Burdick, J. A. Anisotropic Rod-Shaped Particles Influence Injectable Granular Hydrogel Properties and Cell Invasion. *Adv. Mater.* **2022**, *34* (12), 2109194.

(28) Daly, A. C. Granular hydrogels in biofabrication: recent advances and future perspectives. *Adv. Healthcare Mater.* **2023**, *13*, 2301388.

https://doi.org/10.1021/acssynbio.4c00468
ACS Synth. Biol. 2024, 13, 3668−3676